

Experimental investigations of a magnetically driven Tornado-like vortex by means of Ultrasound-Doppler Velocimetry

Tobias Vogt, Ilmars Grants, Sven Eckert and Gunter Gerbeth

Institute of Fluid Dynamics, Helmholtz-Zentrum Dresden-Rossendorf, PO Box 510119,
01314 Dresden, Germany



The spin-up of a concentrated vortex in a liquid metal cylinder with a free surface is considered experimentally. The vortex is driven by two flow independent magnetic body forces. A continuously applied rotating magnetic field provides the source of the angular momentum. A pulse of about one order of magnitude stronger travelling magnetic field drives a converging flow that temporarily focuses this angular momentum towards the axis of the container. A highly concentrated vortex forms that produces a funnel-shaped surface depression. In this study we have used some modified settings for the UDV device in order to detect the vertical position of the free surface along the beam line. The main modification was a reduction of the echo detection sensitivity. In this way the echo from microscopic particles was blinded out. Instead, only the position of the strong echo from the free surface was detected and recorded. We explore experimentally the duration, the depth and the conditions of formation of this funnel.

Keywords: geophysical and geological flow, rotating flows, vortex dynamics, magnetohydrodynamics

1 INTRODUCTION

If a converging flow is superimposed with a far field rotation, the fluid in the convergence zone experiences a strong swirl accumulation due to the angular momentum conservation. This phenomenon, which is also known as vortex stretching, is responsible for spectacular flows like tornadoes [1-3] and tropical cyclones [4-5]. Because of their destructive nature, there is great interest in understanding this flow phenomenon and, thus, a vast literature is available. However, there are comparatively few laboratory experiments. We present an experimental setup and a measuring approach which allows for the generation and analysis of a Tornado-like vortex in a liquid metal bath.

2 EXPERIMENTAL SETUP

The experiments were performed in cylindrical containers which were filled with the low melting temperature eutectic alloy GaInSn ($T_0 = 10.5 \text{ }^\circ\text{C}$). At room temperature, this alloy has a viscosity of $\nu = 3.4 \times 10^{-7} \text{ m}^2 \text{ s}^{-1}$, a density of $\rho = 6.36 \times 10^3 \text{ kg m}^{-3}$ and an electrical conductivity of $\sigma = 3.2 \times 10^6 \text{ S m}^{-1}$. Two cylindrical Perspex containers were used. The smaller cylinder has a diameter of $D_0 = 2R_0 = 60 \text{ mm}$ and is filled up to a height of $H_0 = 60 \text{ mm}$ with the liquid metal. The larger cylinder has a diameter of $D_0 = 2R_0 = 170 \text{ mm}$ and is filled up to a height of $H_0 = 170 \text{ mm}$. Hence, the aspect ratio of the liquid metal in both cylinders was $A = H_0/2R_0 = 1$. In order to avoid oxidation, the free surface of the liquid metal is covered in both cylinders with $\sim 1 \text{ mm}$ thick layer of hydrochloric acid. The smaller cylinder was used mainly for velocity measurements, while the

larger one was used for observation of the free surface deformation and detection of the funnel depth.

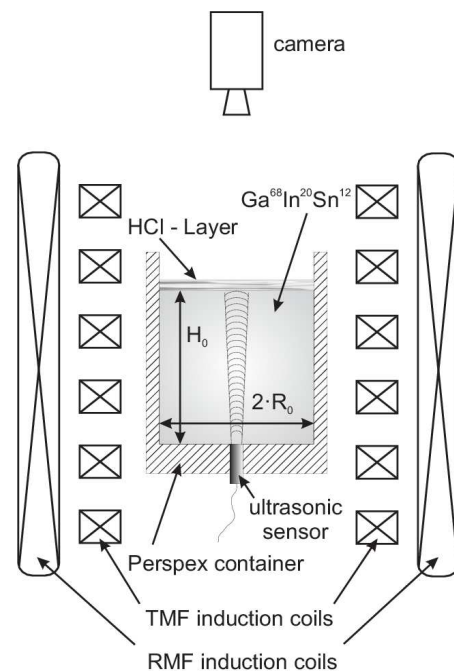


Figure 1: Schematic drawing of the experimental setup

An ultrasound Doppler velocimeter (UDV) (model 2125, Signal Processing SA, Lausanne) was used in the experiments for both the fluid velocity measurements and for the funnel depth detection. In the case of the smaller cylinder, one 8 MHz ultrasound transducer (TR0805LS, acoustic active diameter 5 mm) was attached at the center of the container bottom (see figure 1). In the larger

cylinder, we have attached a 4 MHz transducer (TR0410SS, acoustic active diameter 10 mm) at the bottom of the container whereby the ultrasound beam again coincides with the container axis. Additionally, a video camera was mounted above the container in order to synchronously record the free surface shape. The experiments were carried out in the magnetic induction system PERM at Helmholtz-Zentrum Dresden-Rossendorf (HZDR). It is designed for the combined generation of rotating magnetic fields (RMF) and travelling magnetic fields (TMF) whereby the field parameters B_{RMF} , B_{TMF} , ω_{RMF} and ω_{TMF} can be controlled independently. Under the common low frequency and low induction conditions the RMF and TMF induce magnetic body forces with well-known force distributions [6]. The dimensionless force magnitude of the RMF is given by the magnetic Taylor number:

$$Ta = \frac{\sigma \omega_{RMF} B_{RMF}^2 R_0^4}{\rho \nu^2} \quad (1)$$

The dimensionless magnitude of the TMF induced force is given by:

$$F = \frac{\sigma \omega_{TMF} B_{TMF}^2 \kappa R_0^5}{2 \rho \nu^2} \quad (2)$$

where $\kappa = 21.8 \text{ m}^{-1}$ is the wavenumber of the TMF. The magnetic flux density of both magnetic field B_{RMF} and B_{TMF} in (1) and (2) respectively, is given in terms of the r.m.s. value.

3 RESULTS

The experiments were performed as follows. At the beginning of each measurement the flow was set in motion by the RMF alone for ~ 600 s in order to achieve a stationary background rotation of the liquid metal in the stationary cylinder. The spin-up of the tornado-like vortex starts when a much stronger TMF is switched on additionally to the RMF at $t = 0$ s. An example of a vortex funnel is shown in figure 2. The lifetime of such a vortex funnel was limited to only a few seconds owing to the rapidly upcoming turbulence. The whole spin-up process may be divided into three distinct stages. During the first stage ($t < 1$ s) the poloidal flow accelerated and the free surface remained relatively smooth. During the second stage ($1 < t < 2$ s) the funnel was born at the center of the top surface and grew in depth while its diameter and location remained nearly unchanged. During the third stage ($t > 2$ s) the amplitude and the radial extent of the surface waves grew while the funnel typically moved away from the center in a random direction and finally disappeared. The duration of this final stage was random between 1 and 2 s. Earlier investigations have revealed that a tornado-like vortex depends sensitively on the ratio of the flow circulation to the updraft strength, which is expressed by the swirl ratio.



Figure 2: Snapshot of the free surface showing the tornado-like vortex funnel. $D_0 = 170$ mm; $t = 1,8$ s; $Ta = 1.4 \times 10^7$; $F = 10^{10}$

The ratio of the two magnetic forces Ta/F is analogous to the swirl ratio in our case. The snapshots in figure 3(a–e) display the free surface at $t \approx 1.5$ s for different force ratios $Ta/F = 10$; 14; 25; 50 and 100×10^4 , respectively. These values cover a range of a significant change. The vortex funnel at the low force ratio $Ta/F = 10 \times 10^4$ (figure 3a) was thin and apparently deep. The diameter of the funnel grew with the force ratio (figure 3b,c). At $Ta/F = 50 \times 10^4$ (figure 3d) one can observe the transition to two vortices. When the force ratio was further increased ($Ta/F = 100 \times 10^4$), the number of simultaneously occurring vortices and the radius of their circular path increased. This tendency is illustrated by figure 3(e), where five vortices are seen. These five vortices remained nearly equidistant and travelled on a circular path around the center of the container.

Figure 4 shows the variation of the ultrasound echo strength in time along the beam. Maxima of the echo at the top of these plots mark the position of the macroscopic horizontal reflective surface. A reflective surface below the initial filling level at 170 mm can be either the tip of the funnel or the bottom of smaller cavities this funnel may have spawned. The echo magnitude in figure 4 increases from (a) to (e) due to increasing funnel radius.

The axial velocity measurements are made in the smaller 60 mm container because the reduced cell size results in a much smaller surface deformation and in a longer spin-up. Both effects improve the transient velocity measurement conditions. Figure 5 shows the evolution of the ensemble-averaged vertical velocity profiles along the axis from five repeated measurements. The force ratio was increased from $Ta/F = 0.0037$ to 0.0112 whereby the upwards directed forcing $F = 4.8 \times 10^6$ was kept constant.

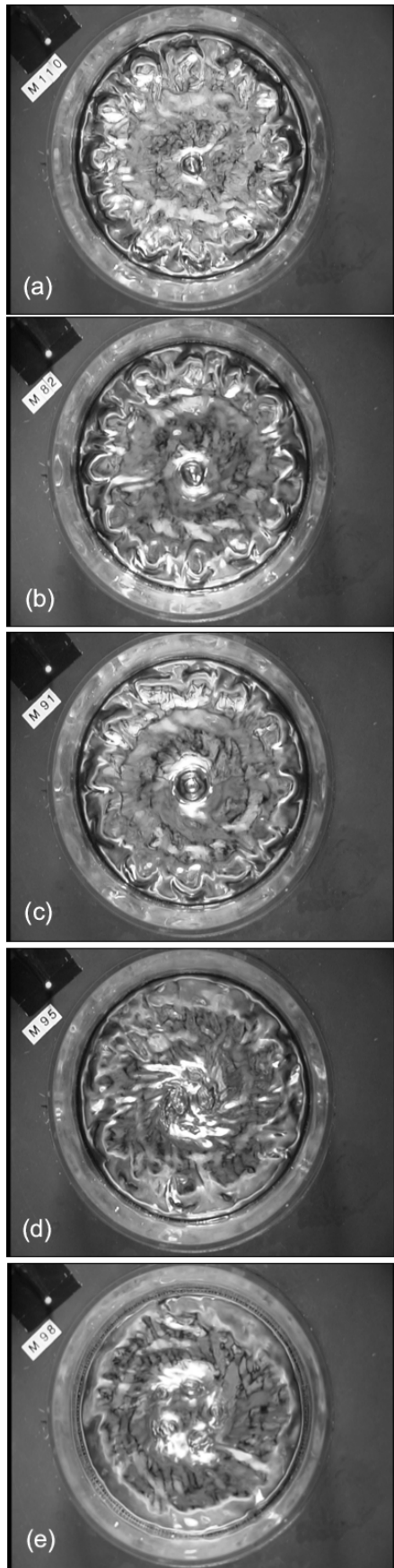


Figure 3: Snapshots of the free surface at $t \approx 1.5$ s. The TMF strength is $F = 6.6 \times 10^9$; the relative RMF strength is $Ta/F = 10, 14, 25, 50$ and 100 ($\times 10^{-4}$) for (a-e) respectively

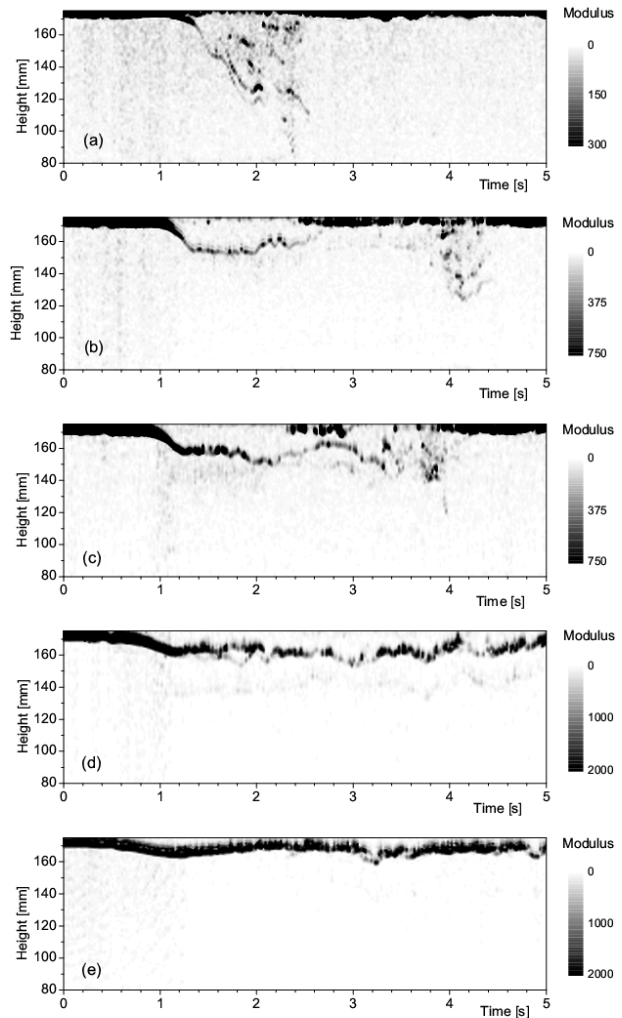


Figure 4: Temporal evolution of profiles of the ultrasound echo modulus. A high value reveals the position of the reflective surface (bottom of the funnel or macroscopic bubble). The magnetic parameters are as in figure 3.

Figure 5 (a) shows the flow at a weak force ratio that does not alter significantly the TMF-alone-driven flow. Figure 5 (b) displays the axial flow at an intermediate force ratio. The downwards directed flow speed during the initial adjustment phase was much lower. At $t \approx 6$ s a region emerged with upwards directed flow. This region quickly spread to about half of the container height. The reason for this counter flow is the breakdown of the concentrated vortex and the accompanied formation of a vortex breakdown bubble. The maximum speed of the upward flow was reached at $t \approx 12$ s. The axial velocity profile did not change significantly during the initial 6 s (figure 5c) when the force ratio was further increased. Afterwards, however, the upwards directed flow region and thus the vortex breakdown bubble expanded to the top surface at $t \approx 10$ s.

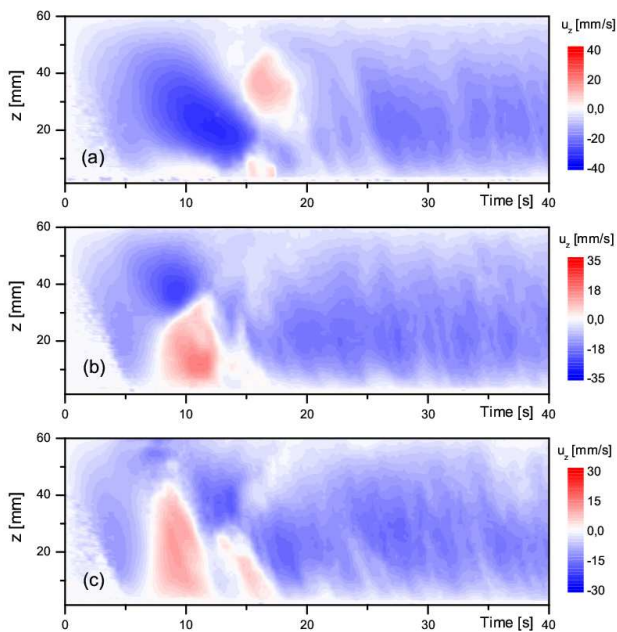


Figure 5: Measurement of the ensemble-averaged vertical velocity distribution along the vessel axis at different force-ratios. (a) $Ta/F = 0.0037$; (b) $Ta/F = 0.0072$; (c) $Ta/F = 0.0112$

In order to estimate the instant of the turbulence onset we have calculated the transient standard deviation of individual measurements (figure 6) from their ensemble-average profiles shown in figure 5. Each standard-deviation plot in this figure was calculated from five measurements. In all three cases displayed in figure 6 the loss of repeatability occurred at about $t = 8-15$ s, whereby the standard deviation generally increases with increasing $Ta=F$.

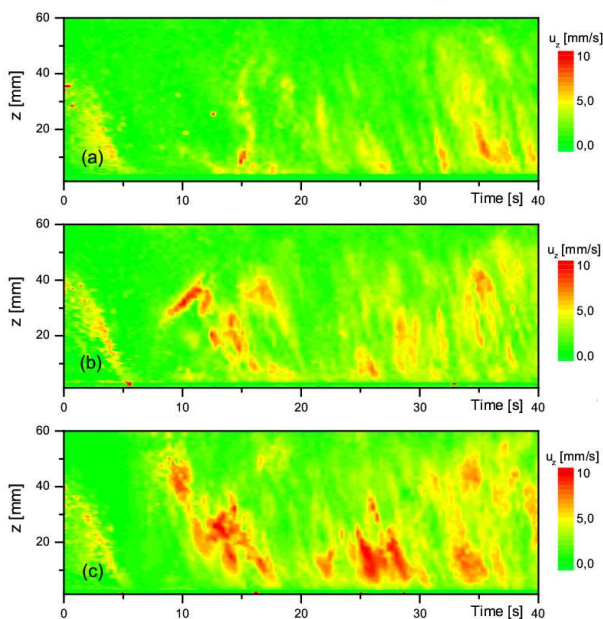


Figure 6: Standard deviation of the averaged vertical velocity distribution at different force-ratios corresponding to figure 5

Some congruent downward trending peaks were observed from $t = 0$ to 5 s. We suspect that those peaks are artefacts connected to low fluid velocities (cf. figure 5) at the beginning of the measurements.

4 SUMMARY

A pulse of TMF produces an intense transient tornado-like vortex in a liquid metal cylinder set in rotation by RMF of an appropriate strength. Being strong enough, such a vortex creates a reproducible sharp funnel at the free surface. The funnel is disrupted by violent turbulence which sets in after the laminar spin-up phase. There are two distinct regimes controlled by the strength of the RMF. For a weak RMF the swirl is much weaker than the meridional flow and it increases with Ta while the vortex width stays independent of RMF. The vortex breakdown, if any, is limited to the lower half of the cylinder. For a strong RMF the swirl intensity stays nearly constant at $\sim F^{1/2}$ while the vortex diameter increases with Ta and the vortex breakdown fills its inner core over the whole height. The Ultrasound-Doppler-velocimeter was used to study the features of the tornado-like vortex. Different setups were used to measure either the vertical velocity distribution along the vessel axis or to detect the vortex funnel depth by means of free surface echo detection. A more detailed description of the performed experiments and the accompanying numerical simulations can be found in [7].

REFERENCES

- [1] Klemp, 1987 Dynamics of tornadic thunderstorms. *Annu. Rev. Fluid Mech.* 19 (1), 369–402.
- [2] Markowski et al., 2008 Vortex lines within low-level mesocyclones obtained from pseudo-dual-Doppler radar observations. *Mon. Weath. Rev.* 136 (9), 3513–3535.
- [3] Rotunno, 2013 The fluid dynamics of tornadoes. *Annu. Rev. Fluid Mech.* 45 (1), 59–84.
- [4] Emanuel, 1991 The theory of hurricanes. *Annu. Rev. Fluid Mech.* 23 (1), 179–196.
- [5] Emanuel, 2003 Tropical cyclones. *Annu. Rev. Earth Planet. Sci.* 31 (1), 75–104.
- [6] Grants et al., 2008 Experimental observation of swirl accumulation in a magnetically driven flow. *J. Fluid Mech.* 616, 135–152.
- [7] Vogt, Grants et al., 2013 Spin-up of a magnetically driven tornado-like vortex. *J. Fluid Mech.* 736 (1) 641-662.